

Quasi-pole quintessential inflation in metric-affine gravity

Konstantinos Dimopoulos,^a Christian Dioguardi,^{b,c}
Ioannis D. Gialamas,^b Antonio Racioppi^b

^aConsortium for Fundamental Physics, Physics Department, Lancaster University, Lancaster LA1 4YB, United Kingdom

^bLaboratory of High Energy and Computational Physics, National Institute of Chemical Physics and Biophysics, R vala pst. 10, Tallinn, 10143, Estonia

^cTallinn University of Technology, Akadeemia tee 23, 12618 Tallinn, Estonia

E-mail: k.dimopoulos@lancaster.ac.uk, christian.dioguardi@kbfi.ee,
ioannis.gialamas@kbfi.ee, antonio.racioppi@kbfi.ee

Abstract. We study quintessential inflation in the framework of metric-affine gravity. It is well known that non-minimal couplings with the Holst invariant can generate a quasi-pole inflationary behaviour resulting in a Starobinsky-like phenomenology. The same quasi-pole behaviour can also be used in order to “flatten” the scalar potential in the Dark Energy era providing a successful framework for quintessential inflation. Agreement with all the observational constraints, reduces the predicted scalar spectral index to a narrow window: $0.966 \lesssim n_s \lesssim 0.967$, making the model highly testable and falsifiable.

Contents

1	Introduction	1
2	The model	3
3	Inflation	4
4	Kination	6
5	Reheating	7
6	Quintessence	8
6.1	First scenario: field freezes before the Dark Energy plateau	9
6.1.1	A brief note on Early Dark Energy	11
6.2	Second scenario: field freezes on the Dark Energy plateau	11
7	Parameter space	13
8	Conclusions	15

1 Introduction

Understanding the accelerated expansion of the Universe at both early [1–4] and late times is one of the central challenges of modern cosmology. The inflationary paradigm provides a compelling explanation for the remarkable homogeneity, isotropy, and flatness of the observable Universe, as well as the nearly scale-invariant spectrum of primordial density perturbations [5–10]. At late times, cosmic acceleration is attributed to Dark Energy, whose simplest realization is a cosmological constant, but requires incredible fine-tuning. This is why dynamical models such as quintessence [11] have been put forward (For a review see Ref. [12]). Such proposals provide a richer and more flexible framework. Despite their successes, these two periods of accelerated expansion are typically described independently, leaving open the question of whether a unified explanation is possible. Moreover, dynamical Dark Energy, such as quintessence, requires an extra tuning, that of initial conditions.

Quintessential inflation gives a natural approach to this problem by using a single scalar field to drive both early- and late-time acceleration [13]. In this framework, the scalar field first dominates the energy density of the Universe during inflation and later reappears as a slowly evolving component that can account for Dark Energy (for recent reviews see Refs. [14, 15]). This unified scenario has the potential to address the coincidence problem and to reduce the number of free parameters compared to separate models for inflation and quintessence while treating both phases of accelerated expansion in a common theoretical framework. It also explains the initial conditions of quintessence, which are determined by the inflationary attractor. Constructing viable quintessential inflation models, however, requires careful control over the scalar potential, as it must support two flat regions: the inflationary plateau and the quintessential tail, while also, allowing for a transition to a kination phase linking the two [16]. Successful quintessential inflation models must account for the

observations of both inflation and Dark Energy, without introducing too many parameters and without significant fine tuning.

The gravitational framework in which the scalar field is embedded plays a crucial role in shaping the dynamics. Metric-affine gravity, where the metric and connection are treated as independent variables, provides a natural setting for introducing non-minimal couplings that can modify the effective scalar-field kinetic term and potential. In particular, couplings to curvature invariants such as the Holst invariant (see [17–42] for recent cosmological applications in this framework) can generate quasi-pole structures in the kinetic function, stretching the potential in field space and producing plateaus suitable for inflation as well as for late-time acceleration. These features allow the construction of models that share some of the attractive properties of α -attractor scenarios, while remaining consistent with quintessential inflation requirements [43–56].

The theoretical appeal of our quintessential framework is further reinforced by recent cosmological observations, which have revitalized the debate surrounding the nature of Dark Energy. While Λ CDM has enjoyed long-standing success, recent BAO measurements from the Dark Energy Spectroscopic Instrument (DESI) DR1 [57] and DR2 [58], combined with CMB and SNe Ia data, exhibit a notable tension with the cosmological constant. Within the standard CPL parametrization [59, 60], $w(a) = w_0 + w_a(1 - a)$, these analyses yield a 3.1σ to 4.2σ preference for a dynamical Dark Energy (DDE) equation of state. Crucially, the best-fit parameters point toward a recent crossing of the “phantom divide” ($w = -1$), suggesting a transition from a phantom regime ($w < -1$) in the past to a quintessence regime ($w > -1$) today.

However, interpreting this phantom crossing as a physical reality warrants caution. From a theoretical standpoint, a true crossing in canonical minimally coupled single-scalar-field models is forbidden by the null energy condition, as it typically introduces ghost instabilities. From an observational perspective, the necessity of such a crossing is highly sensitive to the assumed priors. The rigid linear dependence of the CPL formulation can artificially force a crossing to accommodate low-redshift variations. As demonstrated in [61], extending the parameter space to higher-order CPL expansions or to quintessence like parametrizations [62, 63] can significantly dilute the evidence for DDE, rendering the data consistent with Λ CDM.

Consequently, single-field canonical quintessence remains an exceedingly viable and theoretically sound framework. The DESI data do not definitively mandate a violation of the null energy condition, but rather highlight the potential for a transient, dynamical equation of state with $w \geq -1$. This aligns perfectly with our model, which naturally yields a transient DDE phase as the field freezes on the potential plateau, avoiding the instabilities of phantom models. Thus, quintessence remains a robust alternative, justifying the detailed phenomenological exploration presented herein.

In this work, we present a model of quintessential inflation based on metric-affine gravity non-minimally coupled to the Holst invariant. By appropriately choosing the coupling functions, the model naturally realizes a quasi-pole structure in the kinetic term, giving rise to plateau regions in the scalar potential that support both inflation and Dark Energy. The resulting inflationary predictions closely resemble those of Starobinsky-like models, while the late-time dynamics lead to a frozen or slowly rolling scalar field that can account for the observed Dark Energy density. The model therefore provides a minimal and predictive realization of quintessential inflation, bridging early- and late-time cosmic acceleration within a single coherent framework.

The paper is organized as follows. In section 2 we introduce the model, describing its main features and explaining how the two plateaus, one for inflation and one for Dark Energy, are generated through the Holst term. In section 3 we introduce the well-known formalism for slow-roll inflation and compute the predictions for the CMB observables in our model. In section 4 we discuss kination, a period in which the scalar field kinetic term is the dominant source of the energy density of the Universe. This is a key feature of quintessential inflation models, that allows to put tighter bounds on the parameter space. In section 5 we briefly discuss reheating and explain how the reheating temperature is computed in our model. In section 6 we describe the quintessential predictions of our model by studying the full evolution of the scalar field in presence of radiation and matter fluids. In section 7 we constraint the parameter space and highlight the predictions of our model. Finally, in section 8 we discuss our results comparing it to the available results from Planck [64, 65], Bicep/Keck [66], ACT [67] and DESI [58].

2 The model

We start with the action

$$S = \int d^4x \sqrt{-g} \left[\alpha(\phi) \mathcal{R} + \beta(\phi) \tilde{\mathcal{R}} - \frac{1}{2} (\partial_\mu \phi)^2 - V(\phi) \right], \quad (2.1)$$

where $V(\phi)$ is the scalar potential, and $\alpha(\phi)$ and $\beta(\phi)$ are non-minimal coupling functions. The quantities \mathcal{R} and $\tilde{\mathcal{R}}$ represent, respectively, the Ricci scalar and the Holst invariant (i.e. the contraction of the Riemann curvature with the Levi-Civita antisymmetric tensor), both constructed from an independent connection Γ . Working in the metric-affine framework allows the connection to carry additional dynamics that can be integrated out at the classical level.

After integrating out the independent connection, the theory can be recast into the Einstein frame, where the gravitational sector is of the standard Einstein-Hilbert form. The resulting action reads (see e.g. [17])

$$\mathcal{S} = \int d^4x \sqrt{-\bar{g}} \left[\frac{M_P^2}{2} R - \frac{k(\phi)}{2} (\partial_\mu \phi)^2 - U(\phi) \right], \quad (2.2)$$

where M_P is the reduced Planck mass. All non trivial effects of the original non minimal couplings are now encoded in the non canonical kinetic function $k(\phi)$ and in the Einstein frame potential $U(\phi)$. These are given by

$$k(\phi) = \frac{M_P^2}{2} \left[\frac{1}{\alpha} + \frac{12(\beta \partial_\phi \alpha - \alpha \partial_\phi \beta)^2}{\alpha^2(\alpha^2 + 4\beta^2)} \right], \quad U(\phi) = \frac{V(\phi)}{F^2(\phi)}, \quad F(\phi) = \frac{2\alpha}{M_P^2}. \quad (2.3)$$

For the non-minimal couplings we adopt the choice

$$\alpha(\phi) = \frac{M_P^2}{2} \left(\delta_\alpha^2 + \xi \frac{\phi^2}{M_P^2} \right), \quad \beta(\phi) = \frac{M_P^2}{2} \left(\delta_\beta^2 + \tilde{\xi} \frac{\phi^2}{M_P^2} \right). \quad (2.4)$$

In what follows we impose $\alpha = M_P^2/2$ (i.e. $\delta_\alpha = 1$ and $\xi = 0$), which corresponds to working directly in the Einstein frame and implies $V(\phi) = U(\phi)$. Under this choice the kinetic function simplifies to

$$k(\phi) = 1 + \frac{24\tilde{\xi}^2 \phi^2 M_P^2}{M_P^4 + 4 \left(\delta_\beta^2 M_P^2 + \tilde{\xi} \phi^2 \right)^2}. \quad (2.5)$$

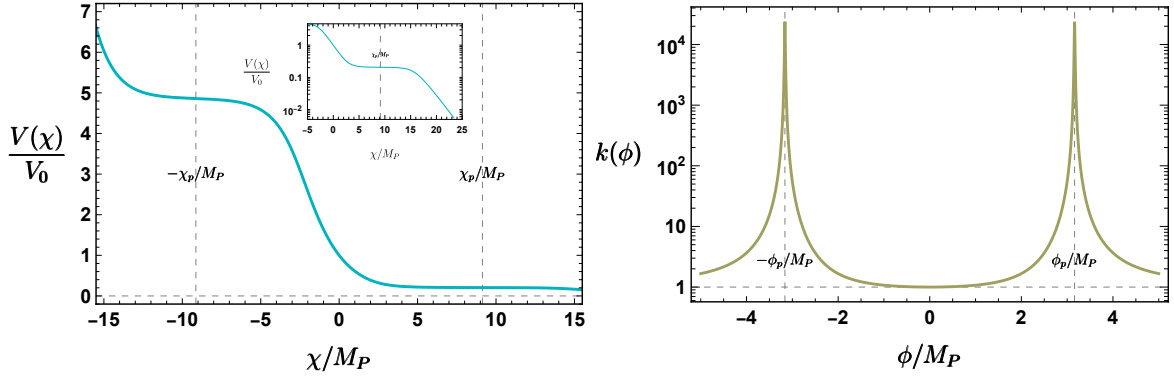


Figure 1: *Left:* The scalar field potential (2.7) as a function of the canonical field χ . The two plateau regions lie in the vicinity of the quasi-pole positions, indicated by the vertical dashed lines. *Right:* The kinetic function $k(\phi)$ given in eq. (2.5) as a function of the scalar field. In both panels, the parameters are $\delta_\beta = 10$, $\tilde{\xi} = -10$, and $\kappa = 1/2$.

This function exhibits a non trivial structure controlled by δ_β and $\tilde{\xi}$. In particular, it possesses a local maximum located at

$$\phi_p^2 = M_P^2 \frac{\sqrt{1 + 4\delta_\beta^4}}{2|\tilde{\xi}|}, \quad \text{with} \quad k(\phi_p) = 1 + 6|\tilde{\xi}| \left(\sqrt{4\delta_\beta^4 + 1} - \text{sign}(\tilde{\xi})2\delta_\beta^2 \right). \quad (2.6)$$

which plays an important role in the dynamics. Although $k(\phi)$ does not develop true poles, for appropriate parameter choices the region around $\pm\phi_p$ can effectively mimic pole like behaviour [30, 41]. From eq. (2.6), we can see that the quasi-pole behaviour is favored when $\tilde{\xi} < 0$, hence, from now on we will adopt such a choice. Note that, after a field redefinition of the form $\sqrt{k(\phi)}d\phi = d\chi$, the kinetic term can be recast into canonical form. In terms of the canonical field, we denote by χ_p the position of the local maximum of the kinetic function $k(\phi)$.

We are interested in exponential potentials of the form

$$V(\phi) = V_0 e^{-\kappa\phi/M_P}, \quad (2.7)$$

where κ is a dimensionless parameter controlling the slope and V_0 sets the overall energy scale and has dimensions of mass⁴. Exponential potentials naturally arise in many high energy constructions [68–70] and are particularly suitable for quintessential inflation scenarios (e.g. [14, 15]).

In figure 1, we show the potential as a function of the canonical field χ and the kinetic function as a function of ϕ . The effect of the quasi poles is clearly visible: near the positions of the quasi-poles the stretched field space flattens the potential, generating extended plateau regions. These plateaus can support slow-roll evolution even when the original potential in ϕ is steep, thereby opening the possibility for successful inflationary and Dark Energy dynamics within a unified setup.

3 Inflation

The inflationary predictions of the model can be computed within the standard slow-roll approximation. After transforming to the canonical field χ , the dynamics is entirely determined

by the Einstein-frame potential $U(\chi)$, so we introduce the usual slow-roll parameters

$$\epsilon(\chi) = \frac{M_P^2}{2} \left(\frac{U'(\chi)}{U(\chi)} \right)^2, \quad \eta(\chi) = M_P^2 \frac{U''(\chi)}{U(\chi)}, \quad (3.1)$$

which quantify, respectively, the slope and curvature of the scalar potential. The duration of inflation is conveniently expressed through the number of e -folds,

$$N_* = \frac{1}{M_P^2} \int_{\chi_{\text{end}}}^{\chi_*} d\chi \frac{U(\chi)}{U'(\chi)}, \quad (3.2)$$

where χ_{end} denotes the field value at the end of inflation, determined by the condition $\epsilon(\chi_{\text{end}}) = 1$. The value χ_* is instead computed by fixing the number of e -folds through [71]:

$$\begin{aligned} N_* = \ln \left(\frac{1}{\sqrt{3}} \left(\frac{\pi^2}{30} \right)^{\frac{1}{4}} \left(\frac{43}{11} \right)^{\frac{1}{3}} \frac{T_0}{H_0} \right) - \ln \left(\frac{k_*}{a_0 H_0} \right) - \frac{1}{12} \ln g_{\text{reh}} \\ + \frac{1}{4} \ln \left(\frac{U_*^2}{M_P^4 \rho_{\text{end}}} \right) + \frac{1-3w}{12(1+w)} \ln \left(\frac{\rho_{\text{reh}}}{\rho_{\text{end}}} \right), \end{aligned} \quad (3.3)$$

and corresponds to the field value at the time at which the pivot scale leaves the horizon. In (3.3) T_0 is the temperature of the universe today, H_0 the Hubble constant, k_* a pivot scale, g_{reh} the number of relativistic degrees of freedom at the time of reheating, U_* the potential at the time when k_* leaves the horizon, $\rho_{\text{end}}, \rho_{\text{reh}}$ the energy density of the universe respectively at the end of inflation and at reheating.

Within the slow-roll approximation, the inflationary observables are directly related to the slow-roll parameters. In particular, the tensor-to-scalar ratio r , the scalar spectral index n_s , and the amplitude of the scalar power spectrum A_s are given by

$$r = 16\epsilon(\chi_*), \quad n_s = 1 + 2\eta(\chi_*) - 6\epsilon(\chi_*), \quad A_s = \frac{1}{24\pi^2 M_P^4} \frac{U(\chi_*)}{\epsilon(\chi_*)}. \quad (3.4)$$

As shown in [41], models described by eq. (2.1) exhibit an attractor behaviour. In particular, the inflationary predictions approach those of Starobinsky inflation independently of the specific form of $V(\phi)$, provided that the function $\beta(\phi)$ possesses a zero and is sufficiently steep in its vicinity. Using eq. (2.4), the attractor regime corresponds to $\delta_\beta \gg 1$, $\tilde{\xi} < 0$ and $|\tilde{\xi}| \gg 1$. In this limit, the inflationary observables admit simple analytic approximations. Following [41], and working at large N_* , δ_β , and $|\tilde{\xi}|$, we obtain

$$r \approx \frac{12}{N_*^2} \left(1 + \frac{N_*^2}{27\gamma^4} \right), \quad (3.5a)$$

$$n_s \approx 1 - \frac{2}{N_*} \left(1 - \frac{N_*^2}{27\gamma^4} \right), \quad (3.5b)$$

$$A_s \approx \frac{\lambda N_*^2}{18\pi^2} \left(1 - \frac{N_*^2}{27\gamma^4} \right), \quad (3.5c)$$

where we have defined

$$\gamma \equiv -\frac{2\delta_\beta \sqrt{|\tilde{\xi}|}}{\kappa} \quad \text{and} \quad \lambda \equiv \frac{V_0}{M_P^4} e^{\frac{\kappa\delta_\beta}{\sqrt{|\tilde{\xi}|}}}. \quad (3.6)$$

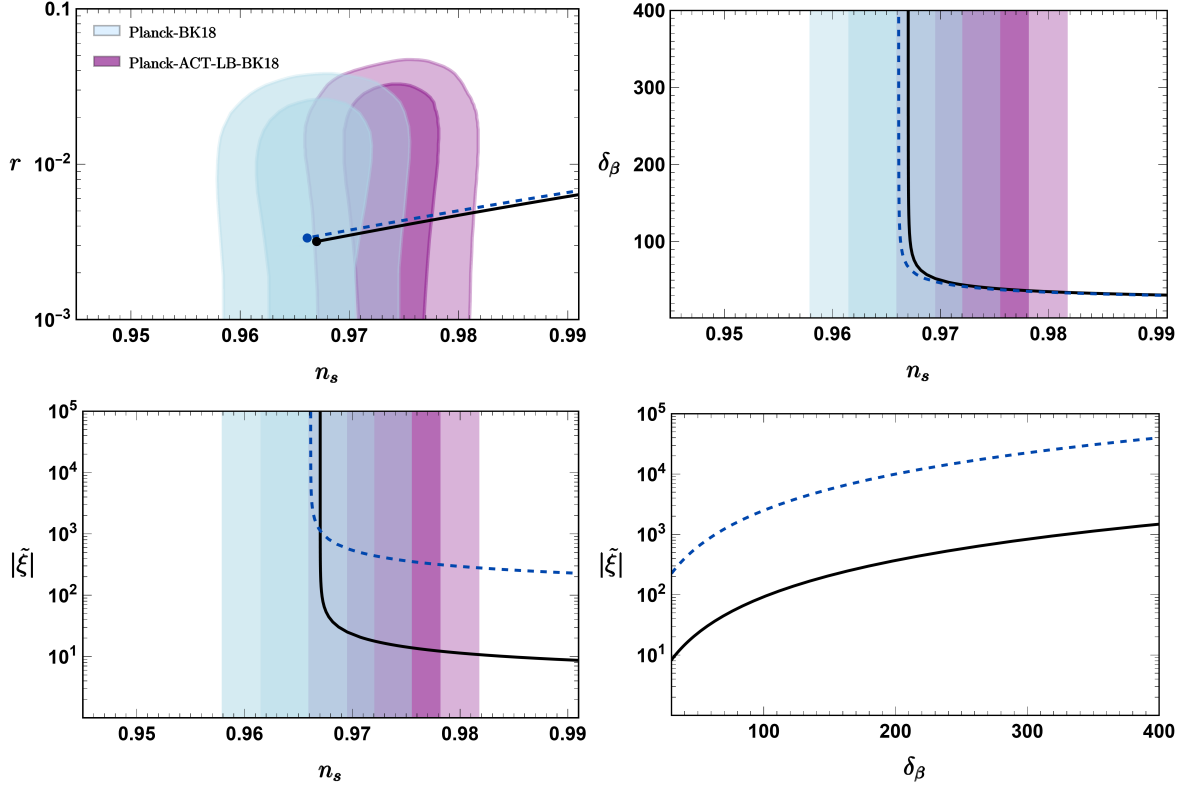


Figure 2: r vs. n_s (top-left), δ_β vs. n_s (top-right), $|\tilde{\xi}|$ vs. δ_β (bottom-left), $|\xi|$ vs. δ_β (bottom-right) for $\phi_p = 2$ at $N_* = 58.9$ (blue, dashed) and $\phi_p = 10.4$ at $N_* = 60.5$ (black, continuous). Since these two models represent two extreme cases for our viable parameter space, the predictions for all other viable sets of ϕ_p and N_* will fall between the two lines. See section 7 for the details on the parameter space, and section 8 for the discussion of the results.

At leading order in the large- γ limit, these expressions reduce to the well-known predictions of Starobinsky inflation. The subleading corrections proportional to γ^{-4} encode the residual dependence on the parameters of the model and quantify the departure from the exact attractor behaviour. As illustrated in Fig. 2, viable parameter choices cluster very close to the Starobinsky predictions, while still allowing for controlled deviations that can be probed observationally.

4 Kinaton

After inflation ends, the Universe naturally enters a period of kinaton, i.e. the kinetic energy of the scalar field becomes the dominant source of energy density of the universe. This period is model independent since the Klein-Gordon equation for the scalar field,

$$\ddot{\chi} + 3H\dot{\chi} + \partial_\chi U(\chi) = 0, \quad (4.1)$$

reduces to

$$\ddot{\chi} + 3H\dot{\chi} \simeq 0, \quad (4.2)$$

because the potential term becomes negligible compared to the Hubble friction and the acceleration terms. The solution of this equation in terms the coordinate time t is given by

$$\dot{\chi} = \sqrt{\frac{2}{3}} \frac{1}{t}. \quad (4.3)$$

As a consequence, the scalar energy density, ρ_χ , evolves as

$$\rho_\chi = \frac{1}{2}\dot{\chi}^2 + U(\chi) \sim \frac{1}{2}\dot{\chi}^2 \propto a^{-6}, \quad (4.4)$$

where $a \propto t^{1/3}$ is the scale factor of the universe during the kination era. Comparing with the general scaling of the continuity equation, $\rho \propto a^{-3(1+w)}$, we deduce that the energy density during kination can be interpreted as the one of a fluid with barotropic parameter $w = 1$. In our model we assume that all radiation is produced at the end of inflation through a mechanism that does not rely on inflaton decay, as we discuss in the next section. Under this assumption, a period of kination generically interpolates between the end of inflation and the onset of radiation domination, which we identify as the reheating time. However, it is a well known fact that kination leads to an enhancement of primordial tensor modes that put a constraint on the duration of kination, N_{kin} , itself. This constraint depends on the tensor-to-scalar ratio, and can therefore be relaxed for those models which provide lower values of r . Moreover, it was recently shown in [72] that kination also amplifies the well-measured amplitude of scalar modes leading to a stricter bound for N_{kin} . Since our model predictions for inflation coincide with the Starobinsky one, we will use the upper bound for kination derived in [72] to constraint our parameter space (see section 7 for the details).

5 Reheating

In the quintessential inflation paradigm, the reheating process differs significantly from standard inflationary scenarios. Since the scalar field must survive to play the role of Dark Energy at late times, it cannot decay into Standard Model (SM) particles in the usual manner. Consequently, the radiation bath required for the Big Bang Nucleosynthesis (BBN) must be generated through alternative mechanisms, such as gravitational reheating [13, 73, 74], instant preheating [75, 76], curvaton reheating [77, 78], Ricci reheating [79–81], reheating by primordial black hole evaporation [82, 83], warm quintessential inflation [84, 85], to name but some.

We define as “reheating” the moment when the energy density of radiation, ρ_r , becomes the dominating source of energy density in the Universe. The efficiency of the reheating process is characterized by the radiation energy density at the end of inflation, ρ_r^{end} . In our framework, this is treated as a free parameter, effectively parameterized by the reheating temperature T_{reh} . Assuming the produced radiation thermalizes sufficiently fast before the onset of the radiation-dominated era, the reheating temperature is given by:

$$T_{\text{reh}} = \left[\frac{30}{\pi^2 g_{\text{reh}}} \left(\Omega_r^{\text{end}} \right)^3 \rho_\chi^{\text{end}} \right]^{1/4}, \quad (5.1)$$

where $g_{\text{reh}} = 106.75$ denotes the number of relativistic degrees of freedom in the SM at high temperatures, and $\Omega_r^{\text{end}} = \rho_r^{\text{end}} / \rho_{\text{tot}}^{\text{end}}$ represents the radiation density parameter at the end of inflation.

The duration of the kination phase, which occurs between the end of inflation and reheating, is crucial for the model’s phenomenological viability. During kination, the scalar energy density redshifts as $\rho_\chi \propto a^{-6}$, while the radiation density redshifts more slowly as $\rho_r \propto a^{-4}$. As a result, lower values of T_{reh} (corresponding to lower Ω_r^{end}) imply a more protracted kination era. This period is subject to several observational constraints: (a) *Scalar and tensor mode enhancement*: A prolonged kination phase can lead to an overproduction of primordial gravitational waves and an enhancement of the scalar power spectrum amplitude. We use the recent bounds derived in Ref. [72] for Starobinsky-like models to establish a lower bound on T_{reh} . (b) *BBN consistency*: To ensure the success of primordial nucleosynthesis, reheating must be completed well before the BBN epoch, imposing the absolute lower limit $T_{\text{reh}} \gtrsim \mathcal{O}(1)$ MeV. (c) *Initial conditions*: We impose the consistency condition $\rho_\chi^{\text{end}} > \rho_r^{\text{end}}$ to ensure that a kination phase actually occurs, which provides a natural upper bound on the reheating temperature.

The specific viable window for T_{reh} in our model, obtained by numerically solving the evolution equations (6.1a)–(6.1d), is discussed in detail in section 7.

6 Quintessence

To extract the quintessential predictions of our model, we numerically track the full background evolution of the scalar field in the presence of radiation and cold dark matter, using the number of e -folds N as the time variable. The dynamics are governed by the first Friedmann equation alongside the continuity equations for the fluid components:

$$3M_P^2 H^2 = (H\chi')^2/2 + U(\chi) + \rho_r + \rho_m, \quad (6.1a)$$

$$H^2 \chi'' + (3H^2 + HH') \chi' = -\partial_\chi U(\chi), \quad (6.1b)$$

$$\rho_r' + 4\rho_r = 0, \quad (6.1c)$$

$$\rho_m' + 3\rho_m = 0, \quad (6.1d)$$

where ρ_r, ρ_m are the energy densities of radiation and cold matter and the $'$ denotes the derivative with respect to N . The initial conditions are set under the assumption that the primordial radiation bath is generated at the end of inflation, while non-relativistic matter is produced during BBN. The initial abundance of radiation is left a priori unconstrained through the choice of T_{reh} . As discussed in section 5, bounds on T_{reh} are self-consistently derived from the phenomenological limits on the duration of the kination epoch. Depending on the parameter space, the quintessential dynamics of our model split into two distinct phenomenological scenarios, illustrated in Figures 3 and 6.

In the **first scenario**, after inflation ends, the field rolls down the exponential potential and freezes during the radiation-dominated era *before* reaching the late-time dark energy plateau. It remains frozen until its energy density becomes comparable to that of the dominant background fluid. Because the relation between ϕ and χ is approximately linear in this intermediate regime, the potential is effectively exponential. Consequently, the scalar field will follow the well-known scaling behavior of exponential quintessence. During this period the scalar field will mimic the barotropic parameter of the dominant fluid and its energy density will be a fixed fraction of the total, i.e.

$$w_\chi = w_B, \quad (6.2)$$

$$\Omega_\chi = \frac{3(1 + w_B)}{\kappa^2}, \quad (6.3)$$

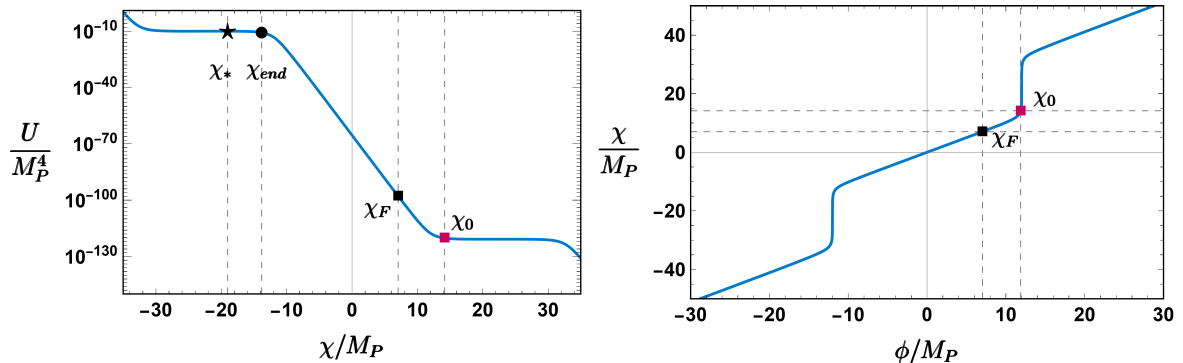


Figure 3: *Left:* Benchmark potential for the first scenario with $|\phi_p| = 12$, $\delta_\beta = 100$, $\tilde{\xi} = -69.5$, $\kappa = 10.633$. The markers indicate critical field values: horizon exit of the pivot scale (χ_* , black star), end of inflation (χ_{end} , black dot), freezing during radiation domination (χ_F , black square), and present day (χ_0 , red square). *Right:* The mapping between the canonical field χ and the original field ϕ . Note that the field freezes while the χ - ϕ relation is still linear.

where w_χ is the barotropic parameter of the scalar field, w_B the barotropic parameter of the dominant background fluid, and $\Omega_\chi \equiv \rho_\chi/\rho_{\text{tot}}$ is the fraction of the energy density of the scalar field to the total energy density of the universe. After entering the scaling behavior the field will start evolving until it reaches the plateau. This will kick the scalar field out of the scaling behavior, allowing it to become the dominant source of energy density of the universe and behave as an effective cosmological constant. Reproducing the observed Dark Energy density requires an appropriate tuning of the potential parameters V_0 and κ . We provide a detailed benchmark for this scenario in section 6.1.

The **second scenario** exhibits qualitatively different late-time dynamics. Here, the field continues to roll down the exponential slope and does not freeze until it has already reached the plateau. Once there, it remains frozen with a nearly constant energy density until it becomes the dominant source of energy density in the Universe. Because the field is already situated on the flat plateau, it bypasses the scaling regime entirely, behaving as a cosmological constant, once it starts dominating. This case is further analyzed in section 6.2.

It is worth noting that in both scenarios, the predicted Dark Energy phase is transient. The finite length of the quintessential plateau in field space implies that, in the far future, the scalar field will eventually roll off the plateau. This will trigger a subsequent kination epoch ($\rho \propto a^{-6}$, $w = 1$), which will ultimately give way to a second matter-dominated phase ($\rho \propto a^{-3}$, $w = 0$).

6.1 First scenario: field freezes before the Dark Energy plateau

We illustrate the first scenario using a benchmark point with $\delta_\beta = 100$, $\tilde{\xi} = -69.5$, and $\kappa = 10.633$ (see Fig. 3, left). The pivot scale exits the horizon at $\chi_* \sim -19.04 M_P$. Inflation unfolds along the first plateau and ends at $\chi_{\text{end}} \sim -13.84 M_P$, accumulating $N_* \sim 59.5$ e -folds. The corresponding CMB predictions are $r \sim 0.0033$ and $n_s \sim 0.9667$. Calibrating the amplitude of the scalar power spectrum to the observed value $A_s \sim 2.1 \times 10^{-9}$ fixes the overall scale $V_0 \sim (108.9 \text{ GeV})^4$, intriguingly close to the electroweak scale. As shown below, this value simultaneously resolves the Dark Energy coincidence problem.

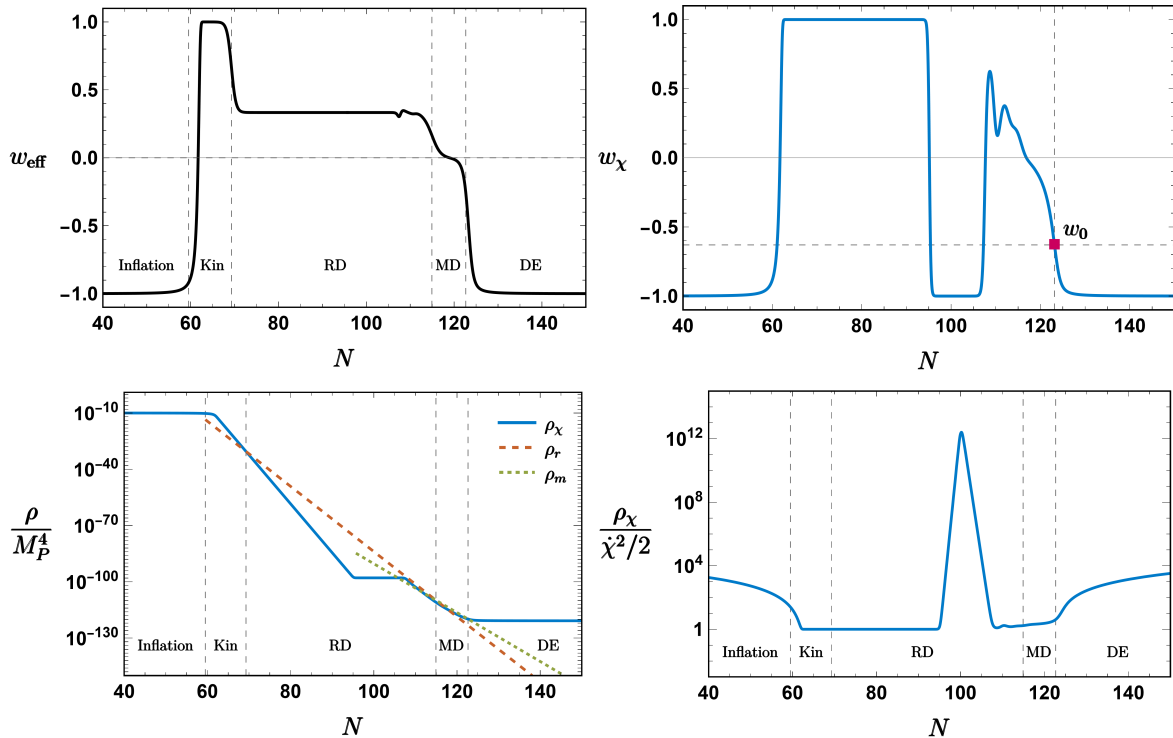


Figure 4: *Top left:* Evolution of the effective equation of state $w_{\text{eff}} \equiv P_{\text{tot}}/\rho_{\text{tot}}$ for the benchmark potential of Fig. 3. *Bottom left:* Evolution of the fractional energy densities for the scalar field (blue), radiation (orange), and cold matter (green). *Top right:* Barotropic parameter of the canonical scalar field. *Bottom right:* Ratio of total to kinetic scalar energy density. The integration starts $N = 40$ e -folds after horizon exit. Today corresponds to $N_0 \sim 123.1$.

Following inflation, a brief kination epoch takes place, lasting $N_{\text{kin}} \sim 9.8$ e -folds. This duration is perfectly compatible with the bounds derived in Ref. [72] for Starobinsky-like inflation. Assuming $g_{\text{reh}} = 106.75$, the associated reheating temperature is $T_{\text{reh}} = 2.3 \times 10^{10}$ GeV.

During radiation domination (RD), the scalar field depletes its kinetic energy and freezes at $\chi_F \sim 7.07 M_P$. As highlighted in Fig. 3 (right), this freezing occurs while the relation between χ and ϕ is still strictly linear, meaning the Einstein-frame potential $U(\chi)$ remains purely exponential. Consequently, the field joins the subdominant scaling attractor, mimicking the background fluid without dominating the energy budget—a well-known hallmark of exponential quintessence. This scaling behavior is visible in Fig. 4 (bottom-left) near the end of the RD era. However, as the field slowly evolves and reaches the second plateau, the χ - ϕ relation becomes non-linear. The presence of the plateau kicks the field out of the scaling regime, initiating the late-time accelerated expansion. At the present epoch ($N_0 \sim 123.1$), the scalar energy density is $\rho_\phi(N_0) \sim 7.15 \times 10^{-121} M_P^4$, with barotropic parameter $w_0 \sim -0.63$, consistent with Dark Energy constraints for dynamical models.

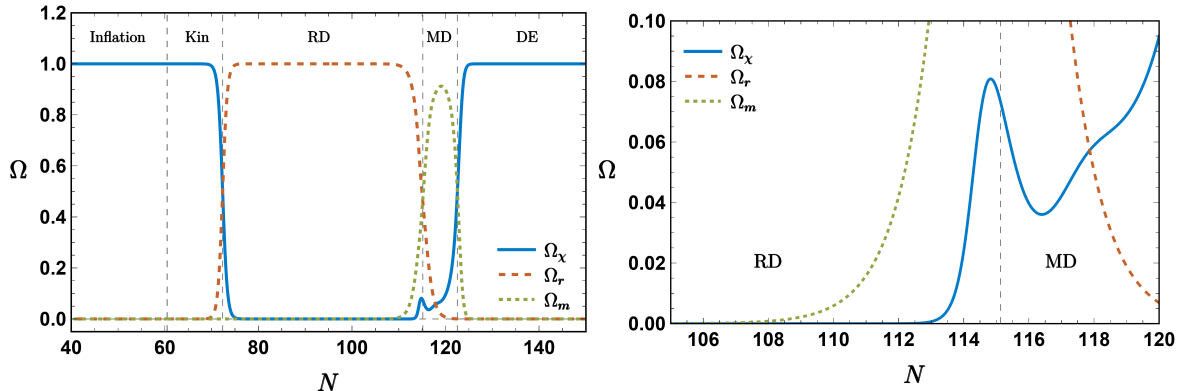


Figure 5: *Left:* Evolution of the density parameters for the scalar field Ω_χ (blue), radiation Ω_r (orange), and cold matter Ω_m (green). *Right:* Magnified view around matter-radiation equality. The transient scaling behavior successfully generates an Early Dark Energy peak comprising $\sim 8\%$ of the total energy budget.

6.1.1 A brief note on Early Dark Energy

Equation (6.2) dictates that the scaling attractor mimics the background fluid’s barotropic parameter, while Eq. (6.3) shows that the field’s fractional energy density remains constant during this regime. As the field enters the scaling solution, its energy density fluctuates. By appropriately tuning κ (or $|\phi_p|$ via Eq. (7.7)) and T_{reh} , it is possible to generate a localized peak in Ω_χ near the epoch of matter-radiation equality. This phenomenological feature is characteristic of Early Dark Energy (EDE) models, which have been proposed to alleviate the H_0 tension when the peak amplitude reaches approximately 10% of the total energy budget [86].

Figure 5 demonstrates this mechanism for a parameter choice of $|\phi_p| = 13.4$ and $T_{\text{reh}} = 1.1 \times 10^9$ GeV. In this realization, the scalar field injects a transient energy density peak of $\sim 8\%$ near N_{eq} . While the peak amplitude is controlled primarily by κ , its temporal location depends sensitively on the initial conditions and T_{reh} . A rigorous parameter estimation via MCMC to determine the viability of this specific EDE realization in resolving the Hubble tension is left for future work.

6.2 Second scenario: field freezes on the Dark Energy plateau

In the second scenario, the field reaches the late-time plateau before freezing. Figure 6 illustrates a benchmark point with $\delta_\beta = 100$, $\tilde{\xi} = -204.1$, $\kappa = 18.142$. Inflation occurs between $\chi^* \sim -14.56 M_P$ and $\chi_{\text{end}} \sim -9.37 M_P$, yielding $N_* \sim 59.5$, $r \sim 0.0032$, and $n_s \sim 0.9667$. A_s is fixed to its observed value $A_s \sim 2.1 \times 10^{-9}$ setting $V_0 \sim (127.1 \text{ GeV})^4$, close to the EW scale. We will see that this value also manages to solve the coincidence problem for Dark Energy.

After the end of inflation the Universe enters a brief kination phase, lasting $N_{\text{kin}} \sim 9.7$ e -folds. Such a duration is fully compatible with the bounds on the kination epoch derived in Ref. [72] for Starobinsky-like inflation. Assuming $g_{\text{reh}} = 106.75$ relativistic degrees of freedom at reheating, the corresponding reheating temperature is $T_{\text{reh}} \sim 2.4 \times 10^{10}$ GeV. During the subsequent radiation-dominated era the scalar field gradually dissipates its kinetic energy and eventually freezes on the plateau of the potential at $\chi_F \sim 11.54 M_P$. This represents a

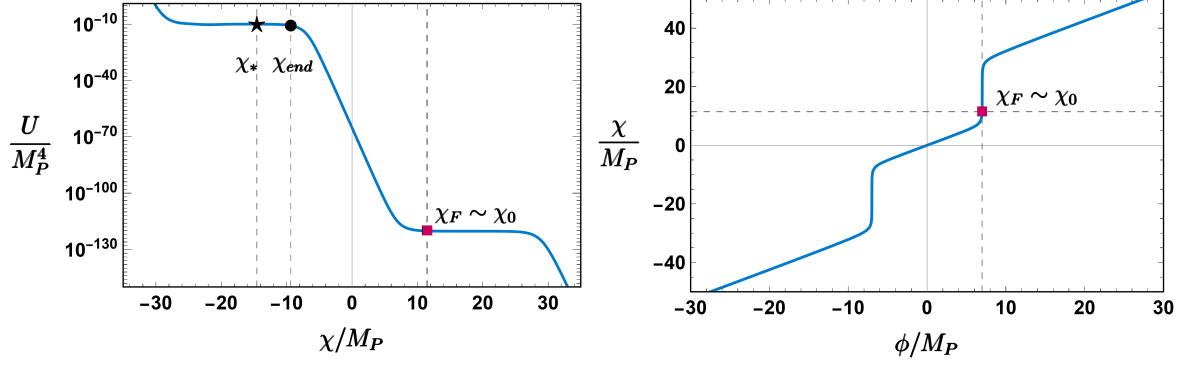


Figure 6: *Left:* Benchmark potential for the second scenario with $|\phi_p| = 7$, $\delta_\beta = 100$, $\tilde{\xi} = -204$, and $\kappa = 18.142$. Markers are the same with those in Fig. 3. *Right:* The mapping between the canonical field χ and the original field ϕ . Note that $\chi_F \sim \chi_0$.

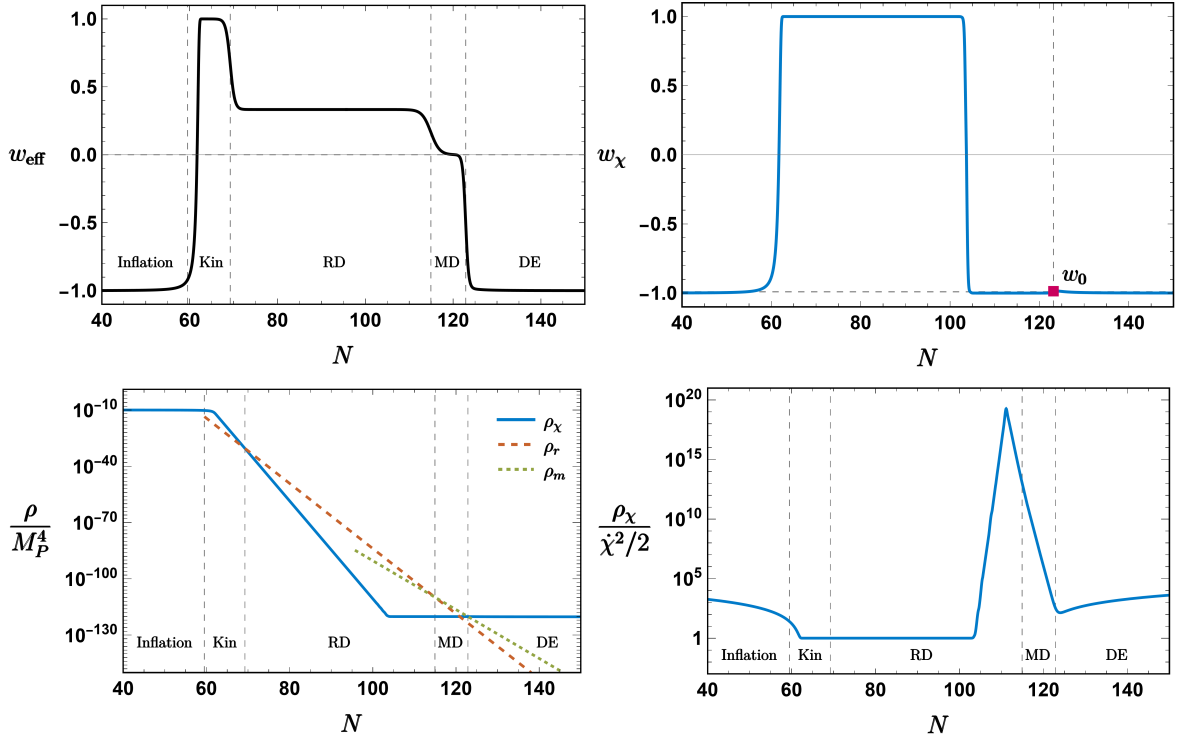


Figure 7: *Top left:* Evolution of w_{eff} for the benchmark potential of Fig. 6. *Bottom left:* Fractional energy densities. *Top right:* Barotropic parameter of the canonical field. *Bottom right:* Ratio of total to kinetic scalar energy density. The field skips the scaling regime entirely, remaining frozen on the plateau. The integration starts $N = 40$ e -folds after horizon exit. Today corresponds to $N_0 \sim 123.1$.

crucial difference with respect to the first scenario, where the field freezes before reaching the plateau. As shown in Fig. 7 (bottom-left), a direct consequence of this behavior is that the scalar field never enters a scaling regime and instead becomes the dominant contribution to the total energy density. At late times the scalar field is therefore dominated by its potential

energy on the plateau and effectively behaves as a cosmological constant. In particular, at $N_0 \sim 123.1$ we find $\rho_\phi(N_0) \sim 7.15 \times 10^{-121} M_P^4$, consistent with the observed Dark Energy density, while the corresponding barotropic parameter is $w_\chi(N_0) \equiv w_0 \sim -0.99$.

7 Parameter space

In this section we constraint the parameter space of our model, spanned by the ‘‘Holst parameters’’ ($\delta_\beta, \tilde{\xi}$), the potential parameters (V_0, κ), the number of inflationary e -folds (N_*), and the reheating temperature (T_{reh}). Using standard values for the pivot scale ($k_* = 0.05 \text{ Mpc}^{-1}$), the Hubble parameter ($H_0 \sim 67.22 \text{ km s}^{-1} \text{ Mpc}^{-1}$), the CMB temperature ($T_0 = 2.725 \text{ K}$), and $g_{\text{reh}} = 106.75$, Eq. (3.3) simplifies to

$$N_* \simeq 61.1 + \frac{1}{4} \ln \left(\frac{U_*^2}{M_P^4 \rho_{\text{end}}} \right) + \frac{1-3w}{12(1+w)} \ln \left(\frac{\rho_{\text{reh}}}{\rho_{\text{end}}} \right). \quad (7.1)$$

Assuming a purely kination-driven transition ($w = 1$) between the end of inflation and reheating, the final term depends solely on the energy density ratios.

Figure 2 displays the predictions for the CMB observables r and n_s . In the strong-coupling limit ($|\tilde{\xi}| \gg 1$), the model accurately recovers the $\tilde{\xi}$ -attractor behavior, continuously approaching the Starobinsky limit as $\delta_\beta \rightarrow \infty$. The black solid line corresponds to $\phi_p = 10.4$ at $N_* \sim 60.5$, yielding $T_{\text{reh}} = 1.1 \times 10^9 \text{ GeV}$ and $N_{\text{kin}} \sim 11.8$. Conversely, the blue dashed line represents $\phi_p = 2$ at $N_* \sim 58.9$, with $T_{\text{reh}} \sim 1.3 \times 10^{11} \text{ GeV}$ and $N_{\text{kin}} \sim 10.1$.

The phenomenological viability of these benchmarks is evaluated against recent constraints on the maximum duration of kination following Starobinsky-like inflation [72], which restrict $N_{\text{kin}} \lesssim 11.8$. Concurrently, a fundamental upper bound on T_{reh} arises from the necessary condition $\rho_\chi^{\text{end}} > \rho_r^{\text{end}}$. This implies $T_{\text{reh}}^{\text{max}} \sim 1.3 \times 10^{11} \text{ GeV}$.

All this induces the following constraints on the parameter space of our model (assuming all radiation is produced at the end of inflation):

$$N_{\text{kin}} \lesssim 11.8, \quad (7.2)$$

$$1.1 \times 10^9 \text{ GeV} \lesssim T_{\text{reh}} \lesssim 1.3 \times 10^{11} \text{ GeV}, \quad (7.3)$$

which correspondingly brackets the allowed number of inflationary e -folds to a narrow window (see eq.(3.3)) given by

$$58.9 \lesssim N_* \lesssim 60.5. \quad (7.4)$$

As depicted in Fig. 2, the lower bound for the parameter δ_β is independent of ϕ_p and hence independent of $\tilde{\xi}$ as well (this happens because all viable models are on the $\tilde{\xi}$ -attractor, i.e. in the $\tilde{\xi} \gg 1$ limit). In particular compatibility with the 2σ region for n_s requires $\delta_\beta \gtrsim 33$ (Planck-ACT-LB-BK18) or $\delta_\beta \gtrsim 38$ (Planck-BK18). The Starobinsky attractor is reached for $\delta_\beta \sim 70$. In this regime, given the narrow window (7.4) we obtain

$$r \sim 0.003 \quad \text{and} \quad 0.966 \lesssim n_s \lesssim 0.967. \quad (7.5)$$

When $\delta_\beta, |\tilde{\xi}| \gg 1$, the relevant parameter for Dark Energy is given by $\phi_p^2 \sim \delta_\beta^2 / |\tilde{\xi}|$. To each $|\phi_p|$ we have a fixed rather fine-tuned value of κ necessary to match the observed value of the Dark Energy density today (smaller ϕ_p require larger κ). We can get an estimation for the potential parameters κ, V_0 by considering the following. The potential $U(\chi)$ in terms of

ϕ_P	N_*	N_{kin}	\bar{T}_{reh} [GeV]	κ	V_0 [GeV]	w_0
2.3	58.9	10.1	1.3×10^{11}	55.305	121.3	-0.946
5.1	59.2	9.8	5.5×10^{10}	24.937	121.3	-0.951
8.8	59.9	10.5	7.2×10^9	14.453	120.3	-0.944
10.4	60.5	11.8	1.1×10^9	12.224	121.4	-0.958

Table 1: Model predictions and required potential parameters for selected values of ϕ_p , computed in the Starobinsky limit ($\delta_\beta, \tilde{\xi} \gg 1$) enforcing $\rho_\chi(N_0) \sim 7.15 \times 10^{-121} M_P^4$. Here, \bar{T}_{reh} denotes the maximum allowed reheating temperature compatible with $-1 \lesssim w_0 \lesssim -0.95$. Temperatures $T_{\text{reh}} > \bar{T}_{\text{reh}}$ push the dynamics into the scaling regime of the first scenario.

the canonical scalar field has a plateau for $\chi \rightarrow \chi_p^-$, where inflation happens, and a plateau for $\chi \rightarrow \chi_p^+$, where we enter late time acceleration. In terms of ϕ this implies that:

$$\begin{cases} U(\phi_p^-) = V_0 e^{-\kappa \phi_p^-} \sim 10^{-10} M_P^4, \\ U(\phi_p^+) = V_0 e^{-\kappa \phi_p^+} \sim 10^{-120} M_P^4, \end{cases} \quad (7.6)$$

yielding

$$V_0 \sim 10^{-65} M_P^4 \sim (100 \text{ GeV})^4 \quad \text{and} \quad \kappa \sim 127/|\phi_p|. \quad (7.7)$$

While these provide excellent initial guesses, precision cosmology requires numerical integration of Eqs. (6.1a)–(6.1d). Table 1 summarizes the exact numerically obtained parameters in the Starobinsky limit.

The parameter space fundamentally dictates the late-time phenomenology:

1) Models with $|\phi_p| \gtrsim 10.4 M_P$ configured for the second scenario require $N_{\text{kin}} \gtrsim 11.8$, and are thus ruled out by the limits discussed in [72]. The limiting case $|\phi_p| \sim 10.4 M_P$ ($N_{\text{kin}} \sim 11.8$, $T_{\text{reh}} \sim 1.1 \times 10^9$ GeV) allows exactly $N_* \sim 60.5$. Forcing more e -folds will imply a lower reheating temperature and larger N_{kin} , which is excluded. Requiring a larger number of e -folds would lead to a lower reheating temperature and a longer kination phase, thereby violating the above bound. Conversely, requiring fewer e -folds increases the reheating temperature and reduces N_{kin} . In this case the scalar field χ freezes before reaching the plateau, which induces the scaling behaviour characteristic of the first scenario. Consequently, models with $|\phi_p| \gtrsim 10.4 M_P$ predict

$$-0.95 \lesssim w_0 \lesssim -0.63. \quad (7.8)$$

2) Models with $|\phi_p| \lesssim 2.3 M_P$, on the other hand, naturally realize the second scenario (for an appropriate choice of V_0 and κ). Since the maximal reheating temperature is bounded by the inflationary plateau, T_{reh} can never become sufficiently large to trigger the first scenario. As a result, for these values of ϕ_p the present-day barotropic parameter lies in the range

$$-1 \lesssim w_0 \lesssim -0.95. \quad (7.9)$$

3) Models with $2.3 M_P \lesssim |\phi_p| \lesssim 10.4 M_P$ admit a maximum reheating temperature \bar{T}_{reh} in the range $1.1 \times 10^9 \text{ GeV} \lesssim \bar{T}_{\text{reh}} \lesssim 1.3 \times 10^{11} \text{ GeV}$, for which the scalar field freezes on the plateau, thereby realizing the second scenario. In these models the prediction $-1 < w_0 \lesssim -0.95$ is obtained only when $1.1 \times 10^9 \text{ GeV} \lesssim T_{\text{reh}} \leq \bar{T}_{\text{reh}}$. Within this range the scalar field effectively behaves as a cosmological constant during the late-time accelerated expansion. The precise

value of \bar{T}_{reh} depends on ϕ_p and must be determined numerically by solving the full scalar-field evolution. In Table 1 we present representative results for several values of ϕ_p , together with the corresponding model parameters and predictions. All benchmark points are computed in the Starobinsky limit $\delta_\beta, \tilde{\xi} \gg 1$, imposing $\rho_\chi(N_0) \sim 7.15 \times 10^{-121} M_P^4$.

8 Conclusions

In this paper, we considered a model of quintessential inflation embedded within the framework of Metric-Affine gravity. We demonstrated how non-minimal couplings to the Holst invariant naturally induce a quasi-pole structure in the effective kinetic term. Upon transforming to the Einstein frame, this geometric stretching generates two distinct, flat plateau regions on a single exponential potential, providing a minimal and theoretically well-motivated mechanism to drive both primordial inflation and late-time cosmic acceleration.

By imposing consistency conditions on the duration of the post-inflationary kination epoch and the onset of radiation domination, we strictly bounded the reheating temperature, restricting the allowed duration of inflation to $58.9 \lesssim N_* \lesssim 60.5$. In the strong-coupling Starobinsky limit ($\delta_\beta \gtrsim 70$), this tightly constrains the scalar spectral index to the narrow, highly predictive window $0.966 \lesssim n_s \lesssim 0.967$. This prediction is in excellent agreement with the Planck-BK18 data [66]. While there is a mild $\sim 2\sigma$ tension with the joint Planck-ACT-LB-BK18 dataset [67], we note that this discrepancy primarily stems from the inclusion of DESI BAO data [58], which introduces a known BAO-CMB tension independent of inflationary physics [87]. Furthermore, improved alignment with the ACT data can be readily achieved outside the strict Starobinsky limit by adopting intermediate coupling values ($35 \lesssim \delta_\beta \lesssim 50$).

At late times, our numerical analysis revealed two viable quintessential regimes. Depending on the geometry of the plateau (ϕ_p) and the thermal history (T_{reh}), the scalar field can either transiently follow a scaling attractor before reaching the Dark Energy plateau (predicting an equation of state with barotropic parameter $-0.95 \lesssim w_0 \lesssim -0.63$, with potential implications for Early Dark Energy), or freeze directly on the plateau, effectively mimicking a pure cosmological constant with $-1 < w_0 \lesssim -0.95$. In both limits, the framework successfully addresses the coincidence problem using natural mass scales ($V_0 \sim \text{TeV}^4$) while unifying the early and late accelerating phases of the Universe.

Acknowledgments

KD was supported (in part) by the Consortium for Fundamental Physics under STFC consolidated grant: ST/X000621/1. This work was supported by the Estonian Research Council grants PSG1132, PRG1677, TARISTU24-TK10, TARISTU24-TK3, and by the CoE program TK202 ‘‘Foundations of the Universe’’. This article is based upon work from COST Action CosmoVerse CA21136, supported by COST (European Cooperation in Science and Technology).

References

- [1] D. Kazanas, *Dynamics of the Universe and Spontaneous Symmetry Breaking*, *Astrophys. J. Lett.* **241** (1980) L59–L63.
- [2] K. Sato, *First Order Phase Transition of a Vacuum and Expansion of the Universe*, *Mon. Not. Roy. Astron. Soc.* **195** (1981) 467–479.

- [3] A. H. Guth, *The Inflationary Universe: A Possible Solution to the Horizon and Flatness Problems*, *Phys. Rev. D* **23** (1981) 347–356.
- [4] A. D. Linde, *A New Inflationary Universe Scenario: A Possible Solution of the Horizon, Flatness, Homogeneity, Isotropy and Primordial Monopole Problems*, *Phys. Lett. B* **108** (1982) 389–393.
- [5] A. A. Starobinsky, *Spectrum of relict gravitational radiation and the early state of the universe*, *JETP Lett.* **30** (1979) 682–685.
- [6] V. F. Mukhanov and G. V. Chibisov, *Quantum Fluctuations and a Nonsingular Universe*, *JETP Lett.* **33** (1981) 532–535.
- [7] S. W. Hawking, *The Development of Irregularities in a Single Bubble Inflationary Universe*, *Phys. Lett. B* **115** (1982) 295.
- [8] A. A. Starobinsky, *Dynamics of Phase Transition in the New Inflationary Universe Scenario and Generation of Perturbations*, *Phys. Lett. B* **117** (1982) 175–178.
- [9] A. H. Guth and S. Y. Pi, *Fluctuations in the New Inflationary Universe*, *Phys. Rev. Lett.* **49** (1982) 1110–1113.
- [10] J. M. Bardeen, P. J. Steinhardt, and M. S. Turner, *Spontaneous Creation of Almost Scale - Free Density Perturbations in an Inflationary Universe*, *Phys. Rev. D* **28** (1983) 679.
- [11] R. R. Caldwell, R. Dave, and P. J. Steinhardt, *Cosmological imprint of an energy component with general equation of state*, *Phys. Rev. Lett.* **80** (1998) 1582–1585, [[astro-ph/9708069](#)].
- [12] E. J. Copeland, M. Sami, and S. Tsujikawa, *Dynamics of dark energy*, *Int. J. Mod. Phys. D* **15** (2006) 1753–1936, [[hep-th/0603057](#)].
- [13] P. J. E. Peebles and A. Vilenkin, *Quintessential inflation*, *Phys. Rev. D* **59** (1999) 063505, [[astro-ph/9810509](#)].
- [14] N. Jaman and M. Sami, *What Is Needed of a Scalar Field If It Is to Unify Inflation and Late Time Acceleration?*, *Galaxies* **10** (2022), no. 2 51, [[arXiv:2202.06194](#)].
- [15] J. de Haro and L. A. Saló, *A Review of Quintessential Inflation*, *Galaxies* **9** (2021), no. 4 73, [[arXiv:2108.11144](#)].
- [16] M. Joyce and T. Prokopec, *Turning around the sphaleron bound: Electroweak baryogenesis in an alternative postinflationary cosmology*, *Phys. Rev. D* **57** (1998) 6022–6049, [[hep-ph/9709320](#)].
- [17] M. Langvik, J.-M. Ojanperä, S. Raatikainen, and S. Rasanen, *Higgs inflation with the Holst and the Nieh–Yan term*, *Phys. Rev. D* **103** (2021), no. 8 083514, [[arXiv:2007.12595](#)].
- [18] M. Shaposhnikov, A. Shkerin, I. Timiryasov, and S. Zell, *Higgs inflation in Einstein–Cartan gravity*, *JCAP* **02** (2021) 008, [[arXiv:2007.14978](#)]. [Erratum: JCAP 10, E01 (2021)].
- [19] M. Piani and J. Rubio, *Higgs-Dilaton inflation in Einstein–Cartan gravity*, *JCAP* **05** (2022), no. 05 009, [[arXiv:2202.04665](#)].
- [20] G. Pradisi and A. Salvio, *(In)equivalence of metric-affine and metric effective field theories*, *Eur. Phys. J. C* **82** (2022), no. 9 840, [[arXiv:2206.15041](#)].
- [21] A. Salvio, *Inflating and reheating the Universe with an independent affine connection*, *Phys. Rev. D* **106** (2022), no. 10 103510, [[arXiv:2207.08830](#)].
- [22] I. D. Gialamas and K. Tamvakis, *Inflation in metric-affine quadratic gravity*, *JCAP* **03** (2023) 042, [[arXiv:2212.09896](#)].
- [23] M. Piani and J. Rubio, *Preheating in Einstein–Cartan Higgs Inflation: oscillon formation*, *JCAP* **12** (2023) 002, [[arXiv:2304.13056](#)].

- [24] I. D. Gialamas and H. Veermäe, *Electroweak vacuum decay in metric-affine gravity*, *Phys. Lett. B* **844** (2023) 138109, [[arXiv:2305.07693](#)].
- [25] A. Di Marco, E. Orazi, and G. Pradisi, *Einstein–Cartan pseudoscalaron inflation*, *Eur. Phys. J. C* **84** (2024), no. 2 146, [[arXiv:2309.11345](#)].
- [26] M. He, M. Hong, and K. Mukaida, *Starobinsky inflation and beyond in Einstein–Cartan gravity*, *JCAP* **05** (2024) 107, [[arXiv:2402.05358](#)].
- [27] A. Racioppi and A. Salvio, *Natural metric-affine inflation*, *JCAP* **06** (2024) 033, [[arXiv:2403.18004](#)].
- [28] T. Inagaki and N. Yoshioka, *Nonthermal particle production in Einstein–Cartan gravity with modified Holst term and nonminimal couplings*, *Phys. Rev. D* **110** (2024), no. 10 103537, [[arXiv:2406.14982](#)].
- [29] I. D. Gialamas and K. Tamvakis, *Inflation in Weyl-invariant Einstein–Cartan gravity*, *Phys. Rev. D* **111** (2025), no. 4 044007, [[arXiv:2410.16364](#)].
- [30] A. Racioppi, $\tilde{\xi}$ -attractors in metric-affine gravity, *JCAP* **04** (2025) 084, [[arXiv:2411.08031](#)].
- [31] I. D. Gialamas and A. Racioppi, *Symmetry-breaking inflation in non-minimal metric-affine gravity*, *JCAP* **05** (2025) 072, [[arXiv:2412.17738](#)].
- [32] G. K. Karananas, *Geometrical origin of inflation in Weyl-invariant Einstein–Cartan gravity*, *Phys. Lett. B* **862** (2025) 139343, [[arXiv:2501.16416](#)].
- [33] T. Katsoulas and K. Tamvakis, *General Einstein–Cartan quadratic gravity with derivative couplings*, *JCAP* **06** (2025) 022, [[arXiv:2502.16980](#)].
- [34] I. D. Gialamas and K. Tamvakis, *Dynamically induced spin-2 mass in a Weyl-invariant framework*, *Phys. Rev. D* **112** (2025), no. 8 084051, [[arXiv:2503.16598](#)].
- [35] A. Salvio, *Independent connection in action during inflation*, *Phys. Rev. D* **112** (2025), no. 6 L061301, [[arXiv:2504.10488](#)].
- [36] I. D. Gialamas, T. Katsoulas, and K. Tamvakis, *Toward a gravitational network: Bridging metric-affine gravity and no-scale supergravity*, *Phys. Rev. D* **112** (2025), no. 9 9, [[arXiv:2506.02159](#)].
- [37] D. Iosifidis, *On the role of the parity violating Hojman–Holst term in gravity theories*, *Phys. Lett. B* **868** (2025) 139705, [[arXiv:2506.04738](#)].
- [38] G. K. Karananas, M. Shaposhnikov, and S. Zell, *Weyl-invariant Einstein–Cartan gravity with a heavy ALP: Higgs inflation and α -attractors*, *Phys. Lett. B* **873** (2026) 140151, [[arXiv:2507.15927](#)].
- [39] G. K. Karananas and M. Shaposhnikov, *Higgs inflation in Weyl-invariant Einstein–Cartan gravity*, [arXiv:2511.04732](#).
- [40] T. Katsoulas and K. Tamvakis, *Inflationary assessment of $F(\mathcal{R}, \tilde{\mathcal{R}})$ Einstein–Cartan models*, [arXiv:2512.02847](#).
- [41] A. Racioppi, *Exponential plateaus and inflation in metric-affine gravity*, [arXiv:2512.16815](#).
- [42] I. D. Gialamas, *Reheating in geometric Weyl-invariant Einstein–Cartan gravity*, [arXiv:2602.00317](#).
- [43] M. W. Hossain, R. Myrzakulov, M. Sami, and E. N. Saridakis, *Variable gravity: A suitable framework for quintessential inflation*, *Phys. Rev. D* **90** (2014), no. 2 023512, [[arXiv:1402.6661](#)].
- [44] C.-Q. Geng, M. W. Hossain, R. Myrzakulov, M. Sami, and E. N. Saridakis, *Quintessential inflation with canonical and noncanonical scalar fields and Planck 2015 results*, *Phys. Rev. D* **92** (2015), no. 2 023522, [[arXiv:1502.03597](#)].

- [45] K. Dimopoulos and C. Owen, *Quintessential Inflation with α -attractors*, *JCAP* **06** (2017) 027, [[arXiv:1703.00305](#)].
- [46] K. Dimopoulos, L. Donaldson Wood, and C. Owen, *Instant preheating in quintessential inflation with α -attractors*, *Phys. Rev. D* **97** (2018), no. 6 063525, [[arXiv:1712.01760](#)].
- [47] Y. Akrami, R. Kallosh, A. Linde, and V. Vardanyan, *Dark energy, α -attractors, and large-scale structure surveys*, *JCAP* **06** (2018) 041, [[arXiv:1712.09693](#)].
- [48] K. Dimopoulos and S. Sánchez López, *Quintessential inflation in Palatini $f(R)$ gravity*, *Phys. Rev. D* **103** (2021), no. 4 043533, [[arXiv:2012.06831](#)].
- [49] L. Aresté Saló, D. Benisty, E. I. Guendelman, and J. de Haro, *α -attractors in quintessential inflation motivated by supergravity*, *Phys. Rev. D* **103** (2021), no. 12 123535, [[arXiv:2103.07892](#)].
- [50] K. Dimopoulos, A. Karam, S. Sánchez López, and E. Tomberg, *Modelling Quintessential Inflation in Palatini-Modified Gravity*, *Galaxies* **10** (2022), no. 2 57, [[arXiv:2203.05424](#)].
- [51] K. Dimopoulos, A. Karam, S. Sánchez López, and E. Tomberg, *Palatini R^2 quintessential inflation*, *JCAP* **10** (2022) 076, [[arXiv:2206.14117](#)].
- [52] T. Inagaki and M. Taniguchi, *Quintessential inflation in logarithmic Cartan $F(R)$ gravity*, *Int. J. Mod. Phys. D* **34** (2025), no. 03 2550005, [[arXiv:2312.11776](#)].
- [53] A. Alho and C. Uggla, *Quintessential α -attractor inflation: a dynamical systems analysis*, *JCAP* **11** (2023) 083, [[arXiv:2306.15326](#)].
- [54] S. Sánchez López, K. Dimopoulos, A. Karam, and E. Tomberg, *Observable gravitational waves from hyperkination in Palatini gravity and beyond*, *Eur. Phys. J. C* **83** (2023), no. 12 1152, [[arXiv:2305.01399](#)].
- [55] W. Giarè, E. Di Valentino, E. V. Linder, and E. Specogna, *Testing α -attractor quintessential inflation against CMB and low-redshift data*, *Phys. Dark Univ.* **46** (2024) 101713, [[arXiv:2402.01560](#)].
- [56] K. Dimopoulos, C. Dioguardi, G. Hütsi, and A. Racioppi, *Quintessential inflation in Palatini $F(R, X)$ gravity*, *Eur. Phys. J. Plus* **140** (2025), no. 11 1109, [[arXiv:2503.21610](#)].
- [57] **DESI** Collaboration, A. G. Adame et al., *DESI 2024 VI: cosmological constraints from the measurements of baryon acoustic oscillations*, *JCAP* **02** (2025) 021, [[arXiv:2404.03002](#)].
- [58] **DESI** Collaboration, M. Abdul Karim et al., *DESI DR2 results. II. Measurements of baryon acoustic oscillations and cosmological constraints*, *Phys. Rev. D* **112** (2025), no. 8 083515, [[arXiv:2503.14738](#)].
- [59] M. Chevallier and D. Polarski, *Accelerating universes with scaling dark matter*, *Int. J. Mod. Phys. D* **10** (2001) 213–224, [[gr-qc/0009008](#)].
- [60] E. V. Linder, *Exploring the expansion history of the universe*, *Phys. Rev. Lett.* **90** (2003) 091301, [[astro-ph/0208512](#)].
- [61] S. Nesseris, Y. Akrami, and G. D. Starkman, *To CPL, or not to CPL? What we have not learned about the dark energy equation of state*, [[arXiv:2503.22529](#)].
- [62] I. D. Gialamas, G. Hütsi, K. Kannike, A. Racioppi, M. Raidal, M. Vasar, and H. Veermäe, *Interpreting DESI 2024 BAO: Late-time dynamical dark energy or a local effect?*, *Phys. Rev. D* **111** (2025), no. 4 043540, [[arXiv:2406.07533](#)].
- [63] I. D. Gialamas, G. Hütsi, M. Raidal, J. Urrutia, M. Vasar, and H. Veermäe, *Quintessence and phantoms in light of DESI 2025*, *Phys. Rev. D* **112** (2025), no. 6 063551, [[arXiv:2506.21542](#)].
- [64] **Planck** Collaboration, Y. Akrami et al., *Planck 2018 results. X. Constraints on inflation*, *Astron. Astrophys.* **641** (2020) A10, [[arXiv:1807.06211](#)].

- [65] **Planck** Collaboration, N. Aghanim et al., *Planck 2018 results. VI. Cosmological parameters*, *Astron. Astrophys.* **641** (2020) A6, [[arXiv:1807.06209](#)]. [Erratum: *Astron. Astrophys.* 652, C4 (2021)].
- [66] **BICEP, Keck** Collaboration, P. A. R. Ade et al., *Improved Constraints on Primordial Gravitational Waves using Planck, WMAP, and BICEP/Keck Observations through the 2018 Observing Season*, *Phys. Rev. Lett.* **127** (2021), no. 15 151301, [[arXiv:2110.00483](#)].
- [67] **Atacama Cosmology Telescope** Collaboration, E. Calabrese et al., *The Atacama Cosmology Telescope: DR6 constraints on extended cosmological models*, *JCAP* **11** (2025) 063, [[arXiv:2503.14454](#)].
- [68] L. Gorlich, S. Kachru, P. K. Tripathy, and S. P. Trivedi, *Gaugino condensation and nonperturbative superpotentials in flux compactifications*, *JHEP* **12** (2004) 074, [[hep-th/0407130](#)].
- [69] M. Haack, D. Krefl, D. Lust, A. Van Proeyen, and M. Zagermann, *Gaugino Condensates and D-terms from D7-branes*, *JHEP* **01** (2007) 078, [[hep-th/0609211](#)].
- [70] Z. Lalak, G. G. Ross, and S. Sarkar, *Racetrack inflation and assisted moduli stabilisation*, *Nucl. Phys. B* **766** (2007) 1–20, [[hep-th/0503178](#)].
- [71] A. R. Liddle and S. M. Leach, *How long before the end of inflation were observable perturbations produced?*, *Phys. Rev. D* **68** (2003) 103503, [[astro-ph/0305263](#)].
- [72] C. Eröncel, Y. Gouttenoire, R. Sato, G. Servant, and P. Simakachorn, *Universal Bound on the Duration of a Kination Era*, *Phys. Rev. Lett.* **135** (2025), no. 10 101002, [[arXiv:2501.17226](#)].
- [73] L. H. Ford, *Gravitational Particle Creation and Inflation*, *Phys. Rev. D* **35** (1987) 2955.
- [74] E. J. Chun, S. Scopel, and I. Zaballa, *Gravitational reheating in quintessential inflation*, *JCAP* **07** (2009) 022, [[arXiv:0904.0675](#)].
- [75] G. N. Felder, L. Kofman, and A. D. Linde, *Instant preheating*, *Phys. Rev. D* **59** (1999) 123523, [[hep-ph/9812289](#)].
- [76] A. H. Campos, H. C. Reis, and R. Rosenfeld, *Preheating in quintessential inflation*, *Phys. Lett. B* **575** (2003) 151–156, [[hep-ph/0210152](#)].
- [77] B. Feng and M.-z. Li, *Curvaton reheating in nonoscillatory inflationary models*, *Phys. Lett. B* **564** (2003) 169–174, [[hep-ph/0212213](#)].
- [78] J. C. Bueno Sanchez and K. Dimopoulos, *Curvaton reheating allows TeV Hubble scale in NO inflation*, *JCAP* **11** (2007) 007, [[arXiv:0707.3967](#)].
- [79] K. Dimopoulos and T. Markkanen, *Non-minimal gravitational reheating during kination*, *JCAP* **06** (2018) 021, [[arXiv:1803.07399](#)].
- [80] T. Opferkuch, P. Schwaller, and B. A. Stefanek, *Ricci Reheating*, *JCAP* **07** (2019) 016, [[arXiv:1905.06823](#)].
- [81] D. Bettoni, A. Lopez-Eiguren, and J. Rubio, *Hubble-induced phase transitions on the lattice with applications to Ricci reheating*, *JCAP* **01** (2022), no. 01 002, [[arXiv:2107.09671](#)].
- [82] I. Dalianis and G. P. Kodaxis, *Reheating in Runaway Inflation Models via the Evaporation of Mini Primordial Black Holes*, *Galaxies* **10** (2022), no. 1 31, [[arXiv:2112.15576](#)].
- [83] M. Riajul Haque, E. Kpatcha, D. Maity, and Y. Mambrini, *Primordial black hole reheating*, *Phys. Rev. D* **108** (2023), no. 6 063523, [[arXiv:2305.10518](#)].
- [84] K. Dimopoulos and L. Donaldson-Wood, *Warm quintessential inflation*, *Phys. Lett. B* **796** (2019) 26–31, [[arXiv:1906.09648](#)].
- [85] J. a. G. Rosa and L. B. Ventura, *Warm Little Inflaton becomes Dark Energy*, *Phys. Lett. B* **798** (2019) 134984, [[arXiv:1906.11835](#)].

- [86] V. Poulin, T. L. Smith, and T. Karwal, *The Ups and Downs of Early Dark Energy solutions to the Hubble tension: A review of models, hints and constraints circa 2023*, *Phys. Dark Univ.* **42** (2023) 101348, [[arXiv:2302.09032](#)].
- [87] E. G. M. Ferreira, E. McDonough, L. Balkenhol, R. Kallosh, L. Knox, and A. Linde, *BAO-CMB tension and implications for inflation*, *Phys. Rev. D* **113** (2026), no. 4 043524, [[arXiv:2507.12459](#)].